DE GRUYTER
OPEN

Beiträge zur Tabakforschung International/
Contributions to Tobacco Research
Volume 26 · No. 6 · June 2015
DOI: 10.1515/cttr-2015-0015

Search for Non-Volatile Components with Low Polarity Characterizing Tobacco Leaves Using Liquid Chromatography / Atmospheric Pressure Chemical Ionization Mass Spectrometry Detector *

by

Naoyuki Ishida

Product Technology Development Center, Japan Tobacco Inc., 1-17-7 Yokokawa, Sumida-ku, Tokyo, Japan

SUMMARY

There has been focus on the components with low polarity in tobacco leaf resin due to their probable relation with taste and aroma of tobacco products, the lack of a feasible analytical method and instrument has long been an obstacle to identifying the components with low polarity. The author thereby paid attention to the analysis employing non-aqueous reversed-phase chromatography hyphenated with a photo diode array detector and an atmospheric pressure chemical ionization mass spectrometry detector which has been considered applicable to the separation of significant but unknown non-volatile. The application succeeded in simultaneously separating, detecting and quantifying more than 100 non-volatile components with different low polarity such as solanesols, triacylglycerols, phytosterols, and chlorophylls. However, their compositional differences among various tobacco leaves still remained partial knowledge based on targeted analysis instead of global knowledge based on comprehensive analysis. No investigation searching for key components elucidating different tastes, aromas, species, cultivars, curing processes, and growing districts among tobacco leaves has been carried out so far. For this reason, all the quantification data were consolidated to form complete multidimensional matrix and were statistically processed to observe the categories and the key components of various tobacco leaves by principal component analysis and hierarchical clustering analysis. Tobacco leaves were first classified into three categories consisting of flue-cured Virginia, air-cured leaf, and Oriental. Solanesyl esters, phytosteryl esters and solanachromene contributed to the category of flue-cured Virginia, while air-cured leaf was characterized by free phytosterols. Oriental was featured by chlorophyll in addition to the contributory components to flue-cured Virginia. Non-volatile components with low polarity seemed to be degraded during curing process and to therefore characterize the different curing processes among various tobacco leaves. [Beitr. Tabakforsch. Int. 26 (2015) 269–283]

KEY WORDS: NARPC; LC/APCI-MSD; non-volatile component with low polarity; resin; tobacco leaf.

ZUSAMMENFASSUNG

Aufgrund ihres wahrscheinlichen Zusammenhangs mit dem Geschmack und Duft von Tabakprodukten wurden Komponenten mit geringer Polarität im Tabakblattharz bisher zwar untersucht, bei der Bestimmung der nicht-flüchtigen Bestandteile mit geringer Polarität war das Fehlen von praktikablen Analysemethoden und -instrumenten jedoch lange ein Hindernis. Der Autor widmete sich daher der

*Received: 21st January 2015 – accepted: 26th May 2015

Analyse dieser Bestandteile unter Verwendung der nichtwässrigen Umkehrphasen-Chromatographie kombiniert mit einem Photodiodenarray-Detektor und einem Massenspektrometrie-Detektor mit chemischer Ionisation bei Atmosphärendruck, die für die Trennung relevanter, aber unbekannter nicht-flüchtiger Bestandteile als geeignet erachtet wurde. Hierdurch gelang die gleichzeitige Trennung, Bestimmung und Quantifizierung von über 100 nichtflüchtigen Bestandteilen mit unterschiedlicher geringer Polarität, wie z.B. Solanesole, Triacylglycerine, Phytosterine und Chlorophylle. Die unterschiedlichen Zusammensetzungen der verschiedenen Tabakblätter blieb jedoch Teilwissen basierend auf einigen gezielten Analysen und nicht Gesamtwissen aus einer umfassenden Analyse. Bislang erfolgten noch keine Untersuchungen der wesentlichen Bestandteile zur Analyse der unterschiedlichen Geschmacksnoten, Düfte, Arten, Sorten, Trocknungsverfahren und Anbauregionen von Tabakblättern. Aus diesem Grund wurden alle Quantifizierungsdaten zur Erstellung einer vollständigen multidimensionalen Matrix konsolidiert und mithilfe der Hauptkomponentenanalyse (PCA) und hierarchischen Clusteranalyse statistisch ausgewertet, um Kategorien und wesentliche Bestandteile verschiedener Tabakblätter zu ermitteln. Die Tabakblätter wurden zunächst in drei Kategorien unterteilt: Flue-cured Virginia (heißluftgetrocknet), air-cured leaf (luftgetrocknete Blätter) und Orienttabak. Solanesylester, Phytosterylester und Solanachromen trugen zur Kategorie des flue-cured Virginia bei, während air-cured leaf durch freie Phytosterine gekennzeichnet war. Orienttabak war zusätzlich zu den ergänzenden Bestandteilen zu flue-cured Virginia charakterisiert durch Chlorophylle. Nicht-flüchtige Bestandteile mit geringer Polarität schienen während des Trocknungsprozesses abgebaut zu werden, so dass sie die unterschiedlichen Trocknungsprozesse bei verschiedenen Tabakblättern charakterisierten. [Beitr. Tabakforsch. Int. 26 (2015) 269–283]

RESUME

Alors que les regards se sont principalement tournés sur les composants à faible polarité dans la résine de feuilles de tabac en raison de leur lien probable avec le goût et l'arôme des produits du tabac, l'absence d'une méthode praticable et d'un outil analytique a longtemps fait obstacle à l'identification des composants non-volatils à faible polarité. L'auteur a, en l'occurrence, porté son attention sur l'analyse recourant à la chromatographie en phase inverse non aqueuse couplée à un détecteur à barrettes de photodiodes et à un détecteur de spectrométrie de masse par ionisation chimique à pression atmosphérique. Cette analyse fut considérée applicable à la séparation des composants non-volatils significatifs mais inconnus. Son application a permis, avec succès, de séparer, détecter et quantifier simultanément plus de 100 composants non-volatils présentant des polarités faibles et différenciées. Ces composantes furent, entre autres, des solanésols, des triacylglycérides, des phytostérols et des chlorophylles. Cependant, les données concernant les différences de composition parmi les diverses feuilles de tabac demeurent encore partielles et basées sur une analyse ciblée plutôt que globales et basées sur une analyse exhaustive. Aucune étude n'a été, à ce jour, accomplie qui recense les composants essentiels permettant de distinguer, parmi les feuilles de tabac, les différents goûts, arômes, variétés, cultivars, processus de séchage et régions de culture. Par conséquent, toutes les données de quantification ont été consolidées dans le but de former une matrice multidimensionnelle complète et ont subi un traitement statistique qui a mis en exergue les catégories et les composants-clés des diverses feuilles de tabac grâce à une analyse en composantes principales et une classification hiérarchique. Les feuilles de tabac ont, dans un premier temps, été ventilées en trois catégories comprenant le tabac jaune de Virginie, les feuilles séchées à l'air et le tabac d'Orient. Les esters de solanésyle, les esters de phytostéryle et le solanachromène ont été recensés dans la catégorie du tabac jaune de Virginie tandis que les feuilles séchées à l'air se sont démarquées par la présence de phytostérols libres. Le tabac d'Orient s'est distingué par sa teneur en chlorophylles, en plus des composants contributifs du tabac jaune de Virginie. Les composants non-volatiles à faible polarité semblent subir une dégradation durant le séchage et donc distinguer les divers processus de séchage des différentes feuilles de tabac. [Beitr. Tabakforsch. Int. 26 (2015) 269–283]

ABRREVIATIONS

The names of components in this manuscript are abbreviated to reduce the number of letters as in the following: Solanesyl esters are abbreviated employing the number of carbon and olefin of intact acid; solanesyl palmitate: Sol-C16; solanesyl linolenate: Sol-C18:3. Triacylglycerols are abbreviated using the initial letters of intact higher fatty acids; linolenic acid: Ln; linoleic acid: L; oleic acid: O; palmitic acid: P; stearic acid: S. A glycerol esterified with P, S and O is abbreviated into OPS. The initial letters of triacylglycerols are alphabetically arranged since positional isomers like sn-2 *vs.* sn-1or -3 positions were not distinguishable in this study. Phytosteryl esters are abbreviated employing the initial letters of intact higher fatty acids in the same manner as solanesyl esters and taking the first five letters of phytosterol moieties; stigmasteryl oleate: O-stigma.

INTRODUCTION

Tobacco leaf, cured *Nicotiana tabacum*, is known for consisting of an elaborate composition of components with different polarities and molecular weights which give unique tastes and aromas to the products (1). There derived a lot of species and cultivars from various cultivation methods and curing processes throughout the world providing region- or manufacturer-specific products (2). The compositional differences derived from such elaborate composition and abundant varieties of tobacco leaves have been considered to be in relation with the taste, aroma, species, cultivars, curing processes, and growing districts (3, 4). For this reason, tobacco leaf components such as terpenoids, lipids, alkaloids, phenylpropanoids, amino

acids, sugars, and even polymers have been qualitatively and quantitatively investigated in detail over the entire year (3–6). Above all, low polar volatile components with less than 300–400 molecular weights such as cembranoids, labdanoids, carotenoids, and lipids included in leaf surface resin have been focused on the most due to their probable relations with taste and aroma (1, 4). Therefore a lot of attention has been paid to their chemical structures, biosynthetic pathways, and plant physiologies (3, 4). On the other hand, non-volatile components with low polarity such as esterified solanesol (Figure 1A) (7, 8) still remained unclear due to the lack of a feasible analytical method.

The cause of the difficulty seems to lie in the structural conformity and large molecular weight of non-volatile components with low polarity.

In the case of esterified solanesol (Figure 1), though its inclusion in tobacco leaf was already confirmed, preliminary hydrolysis of the ester was the exclusive approach used only to clarify the fatty acid composition of the esters (7). Another approach using normal phase liquid chromatography (NPLC) or reversed phase liquid chromatography (RPLC) without preliminary treatment has not accomplished the simultaneous separation, but has provided coeluted esters with similar polarity (9). In addition, gas chromatography (GC) incorporating polar or apolar columns has been unsuitable to volatize solanesyl esters into mass analyzer and has therefore been applied to the analysis of hydrolyzed fatty acids (8, 10). Although a mass filter is able to separate the product ions, an electrospray ionization mass spectrometry detector (ESI-MSD) and atmospheric pressure chemical ionization mass spectrometry detector (APCI-MSD) only provide unidentifiable parent ions ($[M+H^+]^+$) or slightly fragmented ones which are of no help in determining their structures. For these reasons, non-aqueous reversed phase chromatography (NARPC) which is renowned for being able to efficiently separate low polar components without water as eluent became the most promising technique to resolve these problems (11). It was first applied to the separation of lipid and has become a powerful technique with the use of refractive index detector (RID) (12), evaporative light scattering detector (ELSD) (13–15), APCI-MSD (16–22), and atmospheric pressure photoionization mass spectrometer (APPI-MSD) (23).

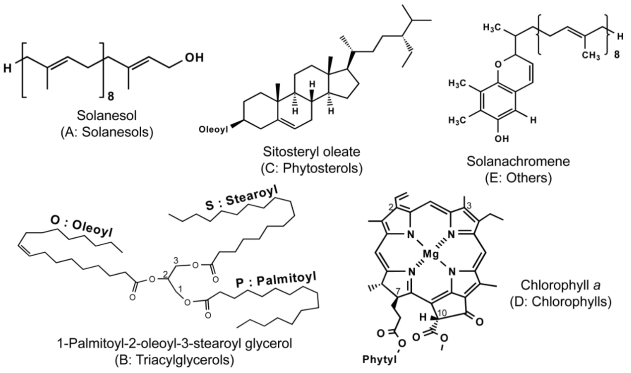

Figure 1. Determined non-volatile components with low polarity in tobacco leaf. The given components are an example of non-volatile components with low polarity classified by component types as in the following; A: Solanesols; B: Triacylglycerols; C: Phytosterols; D: Chlorophylls; E: Others.

NARPC was first applied to the analysis of solanesol and solanesyl esters in tobacco leaf (Figure 1A) (9). The combination with APCI/MSD ensured the chromatographic separation according to the number of carbons and the unsaturated degree of the esters within one run (55 min) without the laborious hydrolysis process. The identification was achieved through the comparison of retention times and spectrum patterns between the authentic components and the analytes. The specific product ions ($[M+H^+$-Acid] gives 613.6 m/z) derived from the elimination of fatty acids generating from the proton adduct ($[M+H^+]$) during ionization process were used for quantifier ions. Since the NARPC showed the sufficient capability of separating non-volatile esters, the application was expanded into the analysis of triacylglycerols in tobacco leaf. Triacylglycerols (Figure 1B) were separated by the simultaneous use of selected ion monitoring (SIM) mode of APCI-MSD within one run (though not separating positional isomers like sn-1, 3 *vs*. sn-2), in which the higher fatty acids of triacylglycerols consisted of linolenic acid <C18:3>, linoleic acid <C18:2>, oleic acid <C18:1>, palmitic acid <C16>, and stearic acid <C18> (24). Their mass spectrums gave diacylglycerol ions ($[M+H^+$-Acid] of 597.5, 599.5 m/z etc.) derived from the elimination of glycerol's higher fatty acid and they were of much help in determining the intact fatty acids. NARPC hyphenated with APCI-MSD was also applied to the analysis of phytosterols and phytosteryl esters in tobacco leaf (25). Four types of phytosterols (cholesterol, campesterol, β-sitosterol and stigmasterol) and 20 phytosteryl esters (Figure 1C) with the above-stated higher fatty acids were simultaneously separated, detected, and quantified. Similar to the case of solanesol and solanesyl esters, specific product ions ($[M+H^+$-Acid] gives 369.4, 383.4 m/z etc.) derived from the elimination of fatty acids from the proton adduct were useful for identification and quantification. The most highlighted application of NARPC to the analysis of non-volatile resin components in tobacco leaf lay in the separation and identification of chlorophylls (Figure 1D) in Oriental (26). While Oriental is harvested in the Mediterranean area (Greece or Turkey) and is renowned for giving a darker green color than flue-cured Virginia and Burley, the causal components of the color have long remained unclear. The simultaneous use of PDAD and APCI-MSD with NARPC worked well on the separation of various tobacco-specific chlorophylls such as solanesyl pheophorbide *a/a'* including a solanesyl group ($C_{45}H_{73}O$) instead of phytyl group ($C_{20}H_{39}O$) at C7 position of chlorophyll *a*, hydroxypheophytin *a/a'* including a hydroxyl group substituted at C10 position as dark green pigments, and solanesyl hydroxypheophorbide *a/a'*.

It would not be an overestimate to say that the preliminarily unknown non-volatile components with low polarity in tobacco leaf have been analyzed enough to determine the key components relating to tastes, aromas, species, cultivars, curing processes, and growing districts among various tobacco leaves. However, these previous studies still remain only partial knowledge based on targeted analysis (9, 24–26) instead of a comprehensive analysis which might produce global knowledge. The genuinely significant components among all ones have remained unclear due to the lack of complete data set consisting of quantification results of each component on each tobacco

leaf. Since the data set becomes available, multivariate analysis such as principal component analysis and hierarchical clustering analysis gets executable. For these reasons, the objective of this study is to search for the key non-volatile components with low polarity elucidating various tobacco leaves through multivariate analysis on first consolidated data matrix.

The initial part of the study is to assign non-volatile components with low polarity on wavelength absorption chromatograms of PDAD and extracted ion chromatograms of APCI/MSD configured at a selected ion monitoring mode to review the previous studies (9, 24–26). The retention times, spectrum patterns, and quantification procedures are summarized in this part. The composition of low polar resins in a tobacco leaf is diagrammatically shown in order to obtain the total image of amounts of each component and to determine the format of data matrix for subsequent multivariate analysis. The normalized data of multidimensional matrix is then subjected to principal component analysis (PCA) and to hierarchical clustering analysis to observe the categories of tobacco leaves. Score plot, clustering and factor loading plot are shown to search for the key components based on comprehensive analysis which might give global knowledge.

MATERIALS AND METHODS

General materials

Flue-cured Virginia (FCV) from Brazil (BRA), Japan (JPN), and Malawi (MWI) harvested between 2005 and 2008; Burley (BLY) from America (USA), Brazil, Italy (ITA), Japan, and Malawi between 2004 and 2010; Oriental (ORI) from Bulgaria (BRG), China (CHN), Greece (GRC), Macedonia (MKD), and Turkey (TUR) between 2005 and 2008; Dark-air cured (DAC) from Brazil and the Philippines (PHI) between 2005 and 2006; Sun-air cured (SAC) from India (IND) between 2004 and 2006. All of these leaves belong to cultivars of *Nicotiana tabacum*. The stem and leaf vein of the tobacco leaves were removed (threshed) prior to analysis except for Oriental. Solvents (acetone, CAS# 67-64-1; acetonitrile, CAS# 75-05-8; *n*-hexane, CAS# 110-54-3; ethyl acetate, CAS# 141-78-6 and ethanol, CAS# 64-17-5) for extraction, purification, and elution were purchased from Wako Pure Chemical Industries, Ltd. (Tokyo, Japan), all of HPLC grade.

Materials for authentic components

In the case of solanesol and solanesyl esters analysis (15), the unavailable authentic esters were synthesized using acids, acid anhydrides, or acyl halides in combination with free solanesol and then were used for identification and quantification. Solanesol, CAS# 13190-97-1 (Sol-OH); heptadecanoyl <C17> chloride, CAS# 40480-10-2; linoleoyl <C18:2> chloride, CAS# 7459-33-8; arachidic <C20> anhydride, CAS# 55726-22-2; behenic <C22> anhydride, CAS# 55726-23-3 and N,N'-dicyclohexylcarbodiimide, CAS# 538-75-0 (DCC) were purchased from Tokyo Chemical Industry Co., Ltd. (Tokyo, Japan). Acetic <C2> anhydride, CAS# 108-24-7; myristoyl <C14> chloride; CAS# 112-64-1, palmitoyl <C16> chloride; CAS# 112-67-4; oleoyl <C18:1> chloride, CAS# 112-77-6; dehydrated pyridine, CAS# 110-86-1 (Py) and 4-dimethylaminopyridine, CAS# 1122-58-3 (DMAP) were purchased from Wako Pure Chemical Industries, Ltd. (Tokyo Japan). Pentadecanoyl <C15> chloride, CAS# 17746-08-6; α-linolenic <C18:3> acid, CAS# 463-40-1 and stearoyl <C18> chloride, CAS# 112-76-5 were purchased from Sigma-Aldrich (St.Louis, MO, USA). Dehydrated tetrahydrofuran, CAS# 109-99-9 (THF) as a solvent for synthesis, was purchased from Kanto Chemical Co., Inc. (Tokyo, Japan).

In the case of triacylglycerols analysis (16), authentic triacylglycerols for identification and simple quantification using response factors were purchased from the following sources: Tripalmitin, CAS# 555-44-2 (PPP) and tristearin, CAS# 68334-00-9 (SSS) were purchased from Wako Pure Chemical Industries, Ltd. (Tokyo Japan); triolein, CAS# 122-32-7 (OOO); trilinolein, CAS# 537-40-6 (LLL) and trilinolenin, CAS# 14465-68 (LnLnLn) were purchased from Sigma-Aldrich (St. Louis, MO, USA).

In the case of free phytosterols and phytosteryl esters analysis (17), the unavailable esters were synthesized in the same procedure as solanesyl esters and were used for identification and quantification. Sitosterol (extracted from soybean oil and including sitosterol (40%), campesterol (27%), stigmasterol (20%) and 2,3-dehydrocampesterol (6%) determined by GC/FID), CAS# 83-46-5 was purchased from Tokyo Chemical Industry Co., Ltd. (Tokyo, Japan). Cholesterol, CAS# 57-88-5 was purchased from Wako Pure Chemical Industries, Ltd. (Tokyo, Japan). Stigmasterol, CAS# 83-48-7 was purchased from TAMA Biochemical Co., Ltd. (Tokyo, Japan). Campesterol, CAS# 474-62-4 and Sitosterol were purified from commercial crude sitosterol using LC/PDAD and were used for reactants identification and quantification. DCC, Py, DMAP, THF, palmitoyl chloride (C16), oleoyl chloride (C18:1), linoleic acid (C18:2), α-linolenic acid (C18:3), and stearoyl chloride (C18) for synthesis were purchased from the same sources as stated in the analysis of solanesols.

In the case of chlorophylls analysis (18), some of the authentic chlorophylls were synthesized through esterification and hydroxylation using the following reagents and were then used for identification and quantification. Chlorophyll *a/a'*, CAS# 479-61-8; chlorophyll *b/b'*, CAS# 519-62-0; pheophytin *a/a'*, CAS# 603-17-8 and pheophytin *b/b'*, CAS# 3147-18-0 were purchased from Wako Pure Chemical Industries, Ltd. (Tokyo Japan). Pheophytin *a/a'* was used for the synthesis of hydroxypheophytin *a/a'* and used for identification and quantification. Pheophorbide *a/a'*, CAS# 15664-29-6 was purchased from Wako Pure Chemical Industries, Ltd. (Tokyo Japan) and was used for the synthesis of solanesyl pheophorbide *a/a'* and Solanesyl hydroxypheophorbide *a/a'*. 1,8-diazabicyclo[5.4.0]undec-7-ene, CAS# 6674-22-2 (DBU); (*1R*)-(+)-(10-camphorsulfonyl) oxaziridine, CAS# 104372-31-8 ((+)-CSOAI) and di-*tert*-butyl dicarbonate, CAS# 24424-99-5 ($(Boc)_2O$) were purchased from Tokyo Chemical Industry Co., Ltd. (Tokyo, Japan). Py, DMAP, THF, and Solanesol were purchased from the same sources as stated in the analysis of solanesols. For the analysis of the other components, β–carotene, CAS# 7235-40-7 and Lutein, CAS# 127-40-2

were purchased from Wako Pure Chemical Industries, Ltd. (Tokyo, Japan). Commercially unavailable Solanachromene was purified from the extract of FCV harvested in the USA. These components were used for identification and quantification.

Preparation of authentic components

Synthesis of solanesyl esters and phytosteryl esters began with stirring these free forms in THF under an argon atmosphere at ambient temperature, and then excessive amounts of Py and a catalytic amounts of DMAP were added and stirred for more than 1 h. When the reactive acylation reagents such as acyl halide were not available, molecularly excessive amount of DCC with catalytic DMAP was added and was stirred until the solution got white. Fatty acids (linolenic and linoleic acid), acid anhydrides (acetic, behenic, and arachidic acid) or acid halides (oleic, palmitic, stearic, myristic, and margaric acid) in THF were added drop by drop to each mixture by a syringe while maintaining the reactant under an argon atmosphere. In the case of using free acid in combination with DCC, the mixture of reactants was thermally refluxed for several hours as necessary. Each reaction was terminated by adding 0.1 M hydrochloric acid aqueous solution, extracted by *n*-hexane three times, washed with saturated sodium chloride water and dried by dehydrated sodium sulfate. Purification of crude reactants was carried out by flash column chromatography (normal-phase eluting *n*-hexane/ethyl acetate for solanesyl esters or *n*-hexane for phytosteryl esters), subsequently another flash column if necessary (reversed-phase eluting acetonitrile/acetone) and recrystallization from collected fractions dissolved by *n*-hexane and ethanol as reported (9, 25). The purities were determined by the given peak areas on full scan analysis of LC/APCI-MSD. The synthesis of solanesyl pheophorbide *a*/*a'* began with dissolving pheophorbide *a* (*a*/*a*' = 85.5/14.5) in dehydrated THF in a two-necked flask filled with argon gas at −42 °C. Excessive amount of dehydrated Py and catalytic amount of DMAP were added and stirred for more than 10 min. $(Boc)_2O$ in THF was added drop by drop to the mixture, 10 min later, solanesol in THF was added. After the solution was stirred for four hours, the reaction was terminated by 0.05 M aqueous hydrochloride, extracted by *n*-hexane three times, washed with saturated sodium chloride water and dried by dehydrated sodium sulfate. The resulting residue was purified by preparative scale thin layer chromatography (normal phase eluting *n*-hexane/ethyl acetate) to give solanesyl pheophorbide *a* (*a*/*a*' = 95.3/4.7 determined by HPLC) as the green component. The synthesis of hydroxypheophytin *a*/*a'* or solanesyl hydroxypheophorbide *a*/*a*' began with dissolving pheophytin *a* (*a*/*a*' = 84.5/15.5) or solanesyl pheophorbide *a* (*a*/*a*' = 95.3/4.7) in THF, and then excessive amounts of DBU was added drop by drop to each reactant. The mixture was stirred at −42 °C for 10 min. Excessive amounts of (+)-CSOAI in THF was added drop by drop to each mixture and stirred for more than four h. Each resultant mixture was handled to give crude reactants in the same procedure as described in the synthesis of solanesyl pheophorbide *a*. The residue was purified by preparative scale thin layer chromatography (normal phase eluting *n*-hexane/ethyl acetate) to give hydroxypheophytin *a* (*a*/*a*' = 38.4/61.6 by HPLC) or solanesyl hydroxypheophorbide *a* (*a*/*a*' = 32.7/67.3 by HPLC) as the dark green component. All procedures were conducted under conditions shielded from light. Purities were determined by the given peak areas on full scan analysis of LC/APCI-MSD (26).

Preparation of tobacco extracts

Approximately 100 g of tobacco leaf was pulverized using an M-2 Mill (Nara Machinery Co., Ltd., Tokyo, Japan) with a 1-mm mesh. It was subsequently subject to an extraction apparatus, ASE200 (Dionex Corporation, Sunnyvale, CA, USA). 2.5 g of pulverized tobacco leaf was inserted in a pressure-resistant vessel (22 mL), which was then filled up with sea sand to remove the air gap. All samples were extracted with about 40 mL of *n*-hexane at 70 °C and 2000 psi. Extracts from 10 g of tobacco leaf (in total four vessels) were carefully transferred to a 250 mL volumetric flask. The applied *n*-hexane extract (10 mL) pipetted by whole pipette was evaporated *in vacuo*, dissolved using acetone, and reapplied to the original volume (10 mL). The acetone solution was filtrated by Millex-LG with a 0.45 µm pore size (Millipore Corporation, Bedford, MA, USA) to remove the insoluble components. The filtrated solution was placed in a tightly sealed glass amber vial in darkness (Agilent Tech., Santa Clara, CA, USA) and was injected into LC/APCI-MSD.

Moisture measurement

Approximately two g of pulverized tobacco leaf was weighed and dried at 80 °C for three h. After drying, it was cooled in a desiccator for an hour and then weighed. The reduction in weight was taken to be the moisture content that was used to evaluate the contents of analytes at dry weight base (D.B.).

Instrumental condition

HPLC analysis in common with all the target components was performed using an Agilent 1200 HPLC system hyphenated with DAD G1315C incorporating 6 mm flow cell G1315-60015 and 6130 APCI/MS (Agilent Tech., Santa Clara, CA, USA). An Excelpak SIL-C18/5C (250 mm × 4.6 mm I.D., 5 µm, Yokogawa Analytical Systems, Japan (currently available from Agilent Tech.)) was used under the following conditions; mobile phase A (acetonitrile), mobile phase B (acetone); flow rate 1.0 mL/min; gradient condition A 100% at 0 min, A 30% at 10 min, A 20% at 30 min, A 0% at 40 min, and A 0% (B 100%) holds until 55 min; column temperature 25 °C. PDAD was configured from 190 to 800 nm of wavelength spectrum, with a 4-mm slit length and 0.1 min of data acquisition frequency and used only for identification and quantification of chlorophyll. Common parameters applied to APCI/MSD without regard to the component types are shown in the following: capillary voltage 4000 V; Corona current 10 µA; drying gas flow 5 mL/min; drying gas temperature 350 °C; fragmentor voltage 200 V; nebulizer pressure 60 psi; vaporizer temperature 500 °C; threshold 150; gain 1.0; step size 0.10; peak width 0.10 min; full-scan

range 100–1850 m/z for identification. All the acquired data was processed with installed software, Chemstation (Agilent Tech., CA, USA). The other parameters for quantification with regard to the component types are described item by item in the following:
In the case of solanesols analysis (9); injection volume: 3 μL; signal measurement period: 10–55 minutes; selected ion: 613.6 m/z; split ratio of flow: 1/13 in front of APCI ionization chamber.
In the case of triacylglycerols (24); injection volume: 50 μL; signal measurement period: 15–55 minutes; selected ion: 551.7, 573.7, 575.7, 577.7, 579.7, 595.7, 597.7, 599.7, 601.7, 603.7, 605.7 and 607.7 m/z.
In the case of phytosterols (25); injection volume: 50 μL; signal measurement period: 10–55 min; selected ion: 369.4, 383.4, 397.4 and 409.4 m/z (10 to 20 min) and then 369.4, 383.4, 395.4 and 397.4 m/z (20 to 55 min); split ratio of flow: 1/4 in front of APCI ionization chamber.
In the case of chlorophylls (26); injection volume: 50 μL; wavelength absorption of PDAD: 660 nm for both identification and quantification. β-carotene, lutein and solanachromene were concurrently analyzed by PDAD configured at 400 nm for carotenoid and 350 nm for solanachromene.

Quantification

Absolute calibration curves of authentic components without regard to component types were drawn by double replication of three levels of standard solutions which inserted about 20 actual analytes in order to decrease the influence of time lapse. Solanesol, solanesyl esters, phytosterols and phytosteryl esters were quantified by the authentic components prepared in advance. Since some of the authentic triacylglycerols observed in tobacco leaf were not available, the triacylglycerols consisting of the same fatty acids such as LnLnLn were used to integrate the intensity of diacylglycerol ion (e.g., $LnLn^+$) derived from the elimination of linolenic acid and then to average two or three different intensities of the diacylglycerol ions to quantify the corresponding triacylglycerol as reported (24) (e.g,. calibration curve of OPS was drawn by the intensities of OP^+, OS^+ and PS^+). Since the quantification of all the determined chlorophylls was difficult to execute, only pheophytin *a* was used as a common authentic component to simply quantify solanesyl pheophorbide *a*/*a*', hydroxypheophytin *a*/*a*' and solanesyl hydroxypheophorbide *a*/*a*' because they give the same wavelength spectrums as pheophytin *a*.

Data processing and multivariate analysis

All quantification data was acquired by triple replication of one extract of each sample and was presented as the average values. All the results were subjected to principal component analysis (PCA) on correlation coefficient matrix and hierarchical clustering analysis on correlation coefficient matrix with a Ward's method for observation of categories of tobacco leaves. All the processes were conducted by a commercial software, JUSE-statworks/V4.0 sw4 (Union of Japanese Scientists and Engineers, Tokyo, Japan).

RESULTS AND DISCUSSION

Identification and quantification of non-volatile components with low polarity

All of the identified components on chromatograms by NARPC hyphenated with PDAD and APCI-MSD are summarized in Figures 2–5 and Table 1. Solanesol and ten types of solanesyl esters including acetic acid, linolenic acid, and behenic acid, etc. were confirmed on the extracted ion chromatogram configured at 613.6 m/z by comparing the separated peaks with the authentic ones (9) (Figure 2).

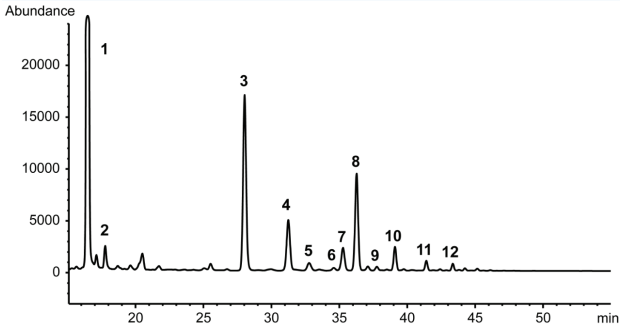

Figure 2. Solanesol and solanesyl esters in tobacco leaf detected by NARPC with APCI-MSD. Chromatogram on SIM mode detecting the fragments $[Solanesol+H^+-H_2O]^+$ and $[Solanesyl\ ester+H^+-Acid]^+$ generated from solanesol and solanesyl esters from the extract of FCV from the USA in 2005. The analytical conditions are described in the "Instrumental condition" of "Materials and methods". Assignment of each component is summarized in Table 1.

The quantification was carried out using preliminarily synthesized solanesyl esters in addition to authentic free solanesol and the method was validated as shown in the following: linearity of calibration curves on all components: >0.999 at the concentrate of 3–800 μg/mL (solanesol) and 0.15–40 μg/mL (solanesyl esters); LOD: 0.024 μg/mL (solanesol) and about 0.01 μg/mL (solanesyl esters); LOQ: 0.080 μg/mL (solanesol) and about 0.1 μg/mL (solanesyl esters); recovery rate: 80–120% on the spiked samples. 35 types of triacylglycerols including Ln, L, O, P and S were determined by SIM mode of APCI-MSD configured at the intense diacylglycerol ions derived from proton adduct triacylglycerol (24) (Figure 3).

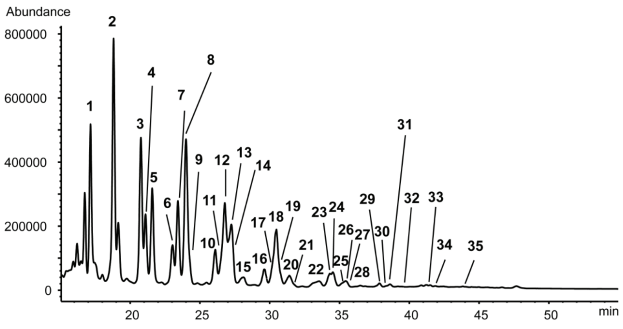

Figure 3. Triacylglycerols in tobacco leaf detected by NARPC with APCI-MSD. Chromatogram on SIM mode detecting the fragments $[Triacylglycerol+H^+-Acid]^+$ from the extract of FCV from the USA in 2005. The analytical conditions are described in the "Instrumental condition" of "Materials and methods". Assignment of each component is summarized in Table 1.

The quantification was conducted by averaged calibration curves calculated from representative triacylglycerols consisting of the same three fatty acids as described in the "Quantification" of "Material and Methods". The validation data showed favorable figures as in the following: linearity of calibration curve on all components: >0.999 at the concentrate of 0.01–6 ng/mL; LOD: about 4 ng/mL; LOQ: about 12 ng/mL; recovery rate: 80–120% on five authentic components.

In the case of phytosterols and phytosteryl esters, four types of phytosterols and 20 types of esters were simultaneously separated and identified by NARPC with APCI-MSD (25) (Figure 4).

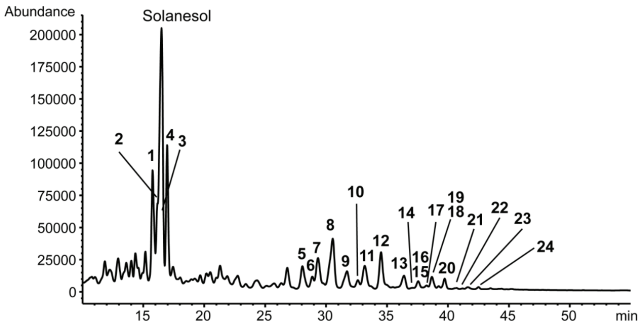

Figure 4. Phytosterols and phytosteryl esters in tobacco leaf detected by NARPC with APCI-MSD. Chromatogram on SIM mode detecting the fragments [Phytosterols+H^+-H_2O]$^+$ and [Phytosteryl esters +H^+-Acid]$^+$ from the extract of ORI from TUR in 2008. The analytical conditions are described in the "Instrumental condition" of "Materials and methods". Assignment of each component is summarized in Table 1.

The most intense product ions derived from the elimination of water or acid molecules from the proton adduct during ionization were used as the quantifier ions. The method was validated as shown in the following: linearity of calibration curve on all components: >0.999 at the concentrate of about 5–20,000 ng/mL; LOD: about 1–3 ng/mL; LOQ: 4–11 ng/mL; recovery rate: 80–120% observed on the spiked samples. Over 20 types of tobacco specific chlorophylls, carotenoids, and solanachromene were separated and identified by NARPC with PDAD and APCI-MSD (26) (Figure 5 not including solanachromene (27)). The steps for determination of chlorophylls began with the assignment of peaks giving the particular wavelength absorption derived from the porphylline skeleton and center magnesium ion (Figure 1D). The firm structures were determined by mass spectrum, retention time, and authentic components. Some of the chlorophylls were quantified by the wavelength absorption of PDAD, because the other chlorophylls were difficult to avail and did not give the desirable intensities for quantification. The quantification was thereby performed by the peak intensity of the pheophytin *a* without a center magnesium ion in order to quantify the chlorophylls giving the similar wavelength spectrum such as hydroxylpheopohytin *a*. The other components such as β-cartotene, lutein, and solanachromene (Figure 1E) were also confirmed on the chromatogram of PDAD and were determined by authentic and isolated components.

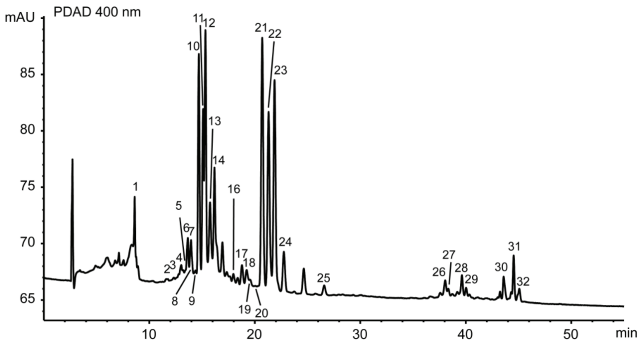

Figure 5. Chlorophyll metabolites in tobacco leaf detected by PDAD with APCI-MSD.
Chromatogram detecting the chlorophyll-specific wavelength absorption from the extract of ORI from TUR in 2008. It also shows the peaks of lutein and β-carotene giving an absorption of 400 nm wavelengths. The analytical conditions are described in the "Instrumental condition" of "Materials and methods". Assignment of each component is summarized in Table 1.

The quantification was at the same time accomplished by PDAD configured at 400 nm for carotenoid and 350 nm for solanachromene (27) in the same manner as chlorophylls. In total, about 100 non-volatile components (Table 1) with low polarity in tobacco leaf were determined and almost all of them were quantified by NARPC hyphenated with PDAD and APCI-MSD providing the complete data set for subsequent multivariate analysis.

Composition of non-volatile components with low polarity

The quantified data results of some tobacco leaves are summarized in Table 2. In order to grasp the whole image of composition of non-volatile components with low polarity, a separately stacked bar chart according to the component types such as solanesol, solanesyl esters, and phytosteryl esters, etc. in FCV from the USA of Table 2 is shown in Figure 6. The largest amount among all was observed in free solanesol of about 1.7% (D.B.)as reported (7). The substantially large amount of each solanesyl esters at concentrations ranging from 100–650 ppm (D.B.) (9) and pigments such as lutein and beta-carotene ranging from 300–600 ppm (D.B.) follows free solanesol. Phytosterols and phytosteryl esters did not give as large an amount as solanesols but reached over 1000 ppm (D.B.) in total in this FCV (25). Each component of chlorophylls gave the lowest amount at the concentrations of 1–3 ppm (D.B.). Although ORI is known for including much larger amounts of these components than FCV and retaining its definitive dark green color (26), since their amounts are less than 30 ppm (D.B.) even in ORI, they seemed to be minor components in comparison with the other quantified. In total, the concentration level against weight of tobacco leaf ranged from ppm to percentile order, which might bring about specific influence of the components with large amounts on multivariate analysis. Therefore, the quantified data result was all normalized among samples and subjected to multivariate analysis in the form of coefficient correlation coefficient matrix.

Table 1. Determined non-volatile components with low polarity in tobacco leaf. The "peak" line stands for the components which were numbered according to retention time on each chromatogram. While the assignment in the table shows the name of determined components, some of them are abbreviated and used in the other figures. The retention times of each component are determined on each chromatogram. The detected wavelengths and mass spectrum ions are given by another scan analysis. The figures in parentheses in the line of wavelength in the table do not stand for the peak value of wavelength but stand for the wavelengths for quantification. The figures with underline in the line of detected ion in the table stand for quantifier ions for SIM mode.

Figure	Peak	Assignment	Abbreviation	Retention time (min)	Detected wavelength (nm)	Detected ion (m/z)	Calibration range (mg/mL)
2	1	Solanesol	Sol-OH	16.47		545.6, 613.6	3.40–838
	2	Solanesyl acetate	Sol-C2	17.79		613.6	0.18–44.0
	3	Solanesyl α-linolenate	Sol-C18:3	28.42		613.6, 891.8	0.15–36.0
	4	Solanesyl linoleate	Sol-C18:2	31.71		545.6, 613.6	0.17–41.0
	5	Solanesyl myristeate	Sol-C14	33.16		545.6, 613.6, 841.8	0.16–40.0
	6	Solanesyl pentadecanoate	Sol-C15	35.02		613.6	0.17–41.0
	7	Solanesyl oleate	Sol-C18:1	35.72		545.6, 613.6, 895.7	0.15–36.0
	8	Solanesyl palmitate	Sol-C16	36.67		545.6, 613.6	0.19–46.0
	9	Solanesyl margrate	Sol-C17	38.14		613.6	0.17–41.0
	10	Solanesyl stearate	Sol-C18	39.47		545.6, 613.6, 897.8	0.18–43.0
	11	Solanesyl arachidinate	Sol-C20	41.77		545.6, 613.6, 925.8	0.17–41.0
	12	Solanesyl behenate	Sol-C22	43.70		545.6, 613.6	0.17–41.0
3	1	Trilinolenin	LnLnLn	17.16		873.7, 595.5	0.01–6.41
	2	Linoleoyl-dilinolenoylglycerol	LLnLn	18.78		875.7, 595.5, 597.5	
	3	Dilinoleoyl-linolenoylglycerol	LLLn	20.76		877.7, 597.5, 599.5	
	4	Dilinolenoyl-oleoylglycerol	LnLnO	21.13		877.7, 595.5, 599.5	
	5	Dilinoleoyl-palmitoylglycerol	LnLnP	21.58		851.8, 573.5, 595.5	
	6	Trilinolein	LLL	23.01		879.8, 599.5	0.01–6.34
	7	Linoleoyl-linolenoyl-oleoylglycerol	LLnO	23.43		879.8, 597.5, 599.5, 601.5	
	8	Linoleoyl-linolenoyl-palmitoylglycerol	LLnP	23.98		853.8, 565.4, 573.5, 597.5	
	9	Dilinolenoyl-stearoylglycerol	LnLnS	24.28		879.8, 595.5, 601.5	
	10	Dilinoleoyl-oleoylglycerol	LLO	26.09		881.7, 599.5, 601.5	
	11	Linolenoyl-dioleoylglycerol	LnOO	26.56		881.7, 599.5, 603.5	
	12	Dilinoleoyl-palmitoylglycerol	LLP	26.78		855.8, 565.4, 599.5	
	13	Linoleoyl-linolenoyl-stearoylglycerol	LLnS	27.13		881.8, 597.5, 601.5, 603.5	
	14	Linolenoyl-oleoyl-palmitoylglycerol	LnOP	27.25		855.8, 573.5, 577.5, 599.5	
	15	Linolenoyl-dipalmitoylglycerol	LnPP	28.05		829.8, 551.5, 573.5	
	16	Linoleoyl-dioleoylglycerol	LOO	29.58		883.8, 601.5, 603.5	
	17	Dilinolenoyl-stearoylglycerol	LLS	30.25		883.8, 599.5, 603.5	
	18	Linoleoyl-oleoyl-palmitoylglycerol	LOP	30.51		857.8, 565.4, 577.5, 601.5	
	19	Linolenoyl-oleoyl-stearoylglycerol	LnOS	30.76		599.5, 601.5, 605.6	
	20	Linoleoyl-dipalmitoylglcerol	LPP	31.36		854.8, 551.5, 565.4	
	21	Linolenoyl-palmitoyl-stearoylglycerol	LnPS	31.61		573.5, 579.5, 601.5	
	22	Triolein	OOO	33.61		603.5	0.01–6.09
	23	Linoleoyl-oleoyl-stearoylglycerol	LOS	34.26		601.5, 603.5, 605.6	
	24	Dioleoyl-palmitoylglycerol	OOP	34.53		577.5, 603.5	
	25	Linoleoyl-palmitoyl-stearoylglycerol	LPS	35.10		565.4, 579.5, 603.5	
	26	Linolenoyl-distearoylglycerol	LnSS	35.20		601.5, 607.6	
	27	Oleoyl-dipalmitoylglycerol	OPP	35.45		577.5, 551.5	
	28	Tripalmitin	PPP	36.45		551.5	0.01–6.12
	29	Dioleoyl-stearoylglycerol	OOS	37.80		603.5, 605.6	
	30	Linoleoyl-distearoylglycerol	LSS	38.36		603.5, 607.6	
	31	Oleoyl-palmitoyl-stearoylglycerol	OPS	38.58		577.5, 579.5, 605.6	
	32	Dipalmitoyl-stearoylglycerol	PPS	39.38		551.5, 579.5	
	33	Oleoyl-distearoylglycerol	OSS	41.30		605.6, 607.6	
	34	Palmitoyl-distearoylglycerol	PSS	41.83		579.5, 607.6	
	35	Tristearin	SSS	43.98		607.6	0.01–6.12

Table 1. contd.

Figure	Peak	Assignment	Abbreviation	Retention time (min)	Detected wavelength (nm)	Detected ion (m/z)	Calibration range (mg/mL)
4	1	Cholesterol		15.64		369.4, 383.4	0.01–35.9
	2	Stigmasterol		16.03		395.4, 409.4	0.01–27.0
	3	Campesterol		16.23		383.4, 397.4	0.01–26.0
	4	Sitosterol		16.83		397.4, 411.4	0.01–25.8
	5	Cholesteryl linolenate	Ln Chole	28.02		369.4	0.01–20.6
	6	Stigmasteryl linolenate	Ln Stigma	28.83		395.4	0.01–21.1
	7	Campesteryl linolenate	Ln Campe	29.31		383.4	0.01–21.2
	8	Sitosteryl linolenate	Ln Sitos	30.54		397.4	0.01–25.5
	9	Cholesteryl linoleate	L Chole	31.71		369.4	0.01–23.0
	10	Stigmasteryl linoleate	L Stigma	32.59		395.4	0.01–21.1
	11	Campesteryl linoleate	L Campe	33.16		383.4	0.01–29.1
	12	Sitosteryl linoleate	L Sitos	34.50		397.4	0.01–21.3
	13	Cholesteryl oleate	O Chole	36.33		369.4	0.00–13.7
	14	Stigmasteryl oleate	O Stigma	37.09		395.4	0.00–16.6
	15	Cholesteryl palmitate	P Chole	37.55		397.4	0.01–32.3
	16	Campesteryl oleate	O Campe	37.59		383.4	0.00–15.5
	17	Stigmasteryl palmitate	P Stigma	38.25		395.4	0.01–28.9
	18	Sitosteryl oleate	O Sitos	38.65		397.4	0.01–22.0
	19	Campesteryl palmitate	P Campe	38.75		383.4	0.01–20.8
	20	Sitosteryl palmitate	P Sitos	39.75		397.4	0.01–25.1
	21	Cholesteryl stearate	S Chole	40.71		369.4	0.01–21.0
	22	Campesteryl stearate	S Stigma	41.25		395.4	0.01–23.5
	23	Campesteryl stearate	S Campe	41.69		383.4	0.01–20.4
	24	Sitosteryl stearate	S Sitos	42.51		397.4	0.01–19.9
5	1	Rutein		8.59	454, 478, (400)		0.38–18.7
	2	Chlorophyll *b*		12.03	456, 594, 644	907.6, 629.2	
	3	Chlorophyll *b*'		12.60	456, 648	907.6	
	4	Chlorophyll *a*		13.14	430, 618, 662	893.5, 615.2	
	5	Chlorophyll *a*'		13.65	664	893.5	
	6	Hydroxypheophytin *b*		13.84	432, 526, 554, 596, 652	901.5, 883.5, 623.4, 605.3	
	7	Hydroxypheophytin *b*'		14.15	434, 526, 554, 596, 652	901.5, 883.5, 623.4, 605.3	
	8	Pheophytin *b*		14.30	434, 526, 550, 596, 652	885.5, 607.4	
	9	Pheophytin *b*'		14.57	434, 652	885.5	
	10	Hydroxypheophytin *a*	OH Pheo a	14.93	406, 502, 530, 608, 664, (400)	887.5, 869.5, 609.4, 591.2	0.35–17.3
	11	Hydroxypheophytin *a*'	OH Pheo a'	15.36	410, 502, 532, 608, 666, (400)	887.5, 869.5, 609.4, 591.2	0.35–17.3
	12	Pheophytin *a*	Pheo a	15.58	408, 504, 534, 608, 664, (400)	871.5, 593.3	0.35–17.3
	13	Pheophytin *a'*	Pheo a'	16.04	408, 502, 534, 608, 666, (400)	871.5, 593.3	0.35–17.3
	14	β-carotene		16.56	446, 474, (400)		0.38–18.7
	15	Solanachromene		18.21	332, (350)	749.6	0.01–21.1
	16	Pyropheophytin *a*		18.31	410, 664	813.8, 535.6	
	17	Solanesyl hydroxypheophorbide *b*		19.18	432, 522, 600, 652	1235.7, 1217.7, 623.3, 605.3	
	18	Solanesyl hydroxypheophorbide *b'*		19.63	434, 522, 600, 652	1235.7, 1217.7, 623.3, 605.3	
	19	Solanesyl pheophorbide *b*		20.01	434, 520, 596, 652	1219.7, 607.4	
	20	Solanesyl pheophorbide *b*'		20.75	436, 652	1219.7, 607.4	
	21	Solanesyl hydroxypheophorbide *a*	Sol OH pheor a	21.19	406, 502, 530, 610, 666, (400)	1221.7, 1203.7, 609.3, 591.2	0.35–17.3
	22	Solanesyl hydroxypheophorbide *a'*	Sol OH pheor a'	21.82	410, 502, 532, 610, 666, (400)	1221.7, 1203.7, 609.3, 591.2	0.35–17.3

Table 1. contd.

Figure	Peak	Assignment	Abbreviation	Retention time (min)	Detected wavelength (nm)	Detected ion (m/z)	Calibration range (mg/mL)
5 contd.	23	Solanesyl pheophorbide *a*	Sol pheor a	22.40	408, 504, 534, 606, 664, (400)	1205.7, 1173.7, 593.3	0.35–17.3
	24	Solanesyl pheophorbide *a*'	Sol pheor a'	23.31	410, 504, 536, 606, 666, (400)	1205.7, 1173.7, 593.3	0.35–17.3
	25	Solanesyl pyropheophorbide *a*		27.26	410, 664	1147.8, 535.6	
	26	Solanesyl hydroxypheophytin *a*		38.63	410, 506, 534, 612, 666	1486.1, 1468.0, 1207.6	
	27	Solanesyl hydroxypheophytin *a*'		38.93	408, 610, 666	1486.1, 1468.0, 1207.6	
	28	Solanesyl pheophytin *a*		40.16	410, 504, 534, 604, 666	1470.1, 857.4, 839.6, 813.6	
	29	Solanesyl pheophytin *a*'		40.54	402, 668	1470.1, 857.4, 839.6, 813.6	
	30	Disolanesyl hydroxypheophorbide *a/a'*		43.96	408, 500, 532, 610, 666	1820.3, 1207.8, 1187.8, 1163.8	
	31	Disolanesyl pheophorbide *a*		44.92	408, 504, 536, 608, 666	1804.4, 1191.8, 1173.8, 1147	
	32	Disolanesyl pheophorbide *a*'		45.30	406, 668	1804.4, 1191.8, 1173.8, 1147.8	

Principal component analysis and hierarchical clustering analysis for key non-volatile component with low polarity

Thirty-eight types of various tobacco leaves described in the"General materials" of "Material and methods" were analyzed and subjected to PCA. The score plot consisting of principal component 1 (34%) and 2 (21%) is shown in Figure 7. The tobacco samples were distributed with some distance and they seemed to be classified into three main categories such as FCV, BLY, and ORI. SAC and DAC were distributed in the category of BLY probably due to the similar air-curing process to BLY. In total, the principal component 1 worked on well in distributing FCV far from air-cured tobacco leaves. On the other hand, the principal component 2 contributed to distributing ORI from the others leaves. Hierarchical clustering analysis on Ward's method was conducted and overwritten on the score plot of PCA to further confirm the categories of tobacco leaves. The dotted lines in Figure 7 showed the same three categories consisting of FCV, air-cured and ORI as in the PCA score plot. In total, non-volatile components with low polarity in tobacco leaves predominantly contributed to the different curing process instead of different growing districts between USA and JPN or and different cultivars between BLY and DAC.

Figure 8 shows the factor loading plot consisting of the same principal components as Figure 7. The coefficient value on the loading plot indicates the significance of the key components contributing to each principal component. Triacylglycerols including unsaturated higher fatty acids (Ln, L and O) were placed at the right side and were considered to contribute to principal component 1. Since the principal component 1 distributed FCV and ORI from BLY, these triacylglycerols were considered to be abundant in lightly cured tobacco leaves like FCV and ORI. While free phytosterols were located at the lower left of the factor loading plot indicating their contributions to BLY, phytosteryl esters, solanesyl esters and solanachromene placed at the upper right strongly contributed to FCV. As solanachromene was expected to generate from under high temperature in curing process like flue-curing (27), its contribution to FCV observed in this plot supported the previous knowledge (27). Moreover, the esterification degree of phytosterols and solanesols seemed to be related to curing process, in which the ester forms were richer in

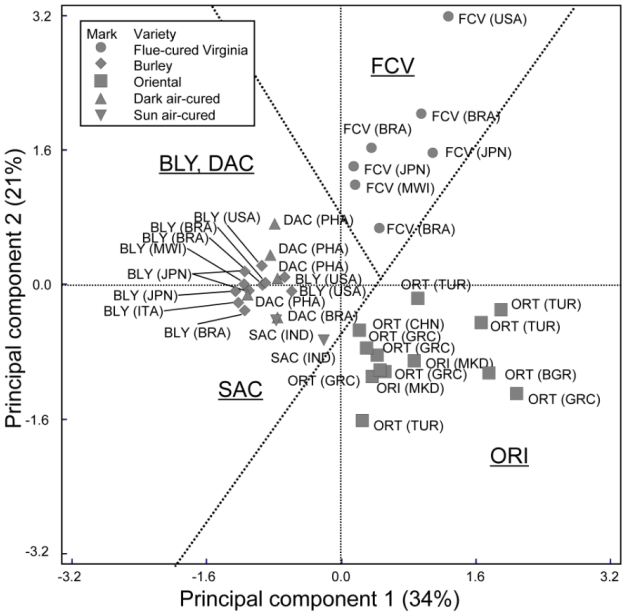

Figure 7. Score plot of principal component analysis of various tobacco leaves. Plot consists of principal component 1 and 2 containing of the largest variance on analysis. The cultivars of tobacco leaves are differently marked to observe the categories. The parenthesis behind the name of cultivar stands for the growing districts in the form of three letters. The dotted lines show the categories given by hierarchical clustering analysis. The details of multivariate analysis are described in the "Data processing and multivariate analysis" of "Materials and methods".

Table 2. Quantification result of non-volatile components with low polarity in tobacco leaf. The "peak" line stands for the components which were numbered according to retention time on each chromatogram. The quantification results are summarized in the right part of the the table and shown in the unit of ppm (D.B.). The abbreviated cultivars and the following growing districts are explained in the "General materials" of "Material and methods". The analytical conditions are described in the "Instrumental condition" of "Material and methods".

Figure	Peak	Assignment	FCV (USA)	FCV (JPN)	BLY (USA)	BLY (JPN)	ORI (GRC)	ORI (TUR)	DAC (PHI)	SAC (IND)
			(ppm (D.B.))							
2	1	Solanesol	16092.0	5429.9	15829.2	12267.1	8958.4	9108.2	4691.1	1398.3
	2	Solanesyl acetate	617.1	32.9	441.0	402.0	147.6	98.4	71.2	36.6
	3	Solanesyl α-linolenate	444.6	311.1	363.5	270.0	867.7	1562.4	558.4	88.0
	4	Solanesyl linoleate	389.4	212.0	426.8	231.6	228.1	309.7	343.7	42.2
	5	Solanesyl myristeate	139.9	55.7	126.9	66.6	54.1	60.6	97.7	16.0
	6	Solanesyl pentadecanoate	22.1	9.5	70.3	42.1	21.8	14.0	51.9	6.7
	7	Solanesyl oleate	151.1	73.2	196.7	58.9	151.2	231.8	410.4	31.8
	8	Solanesyl palmitate	568.2	314.4	452.0	239.3	454.0	681.5	890.8	92.6
	9	Solanesyl margrate	29.0	16.7	33.7	18.8	15.3	20.0	34.3	4.8
	10	Solanesyl stearate	109.7	74.4	88.2	52.5	77.9	131.1	197.1	22.7
	11	Solanesyl arachidinate	66.1	41.1	43.6	25.7	29.0	50.5	70.8	12.7
	12	Solanesyl behenate	56.3	31.3	47.5	22.7	24.7	38.2	65.8	13.7
3	1	Trilinolenin	38.0	61.0	6.2	11.1	36.3	67.8	1.0	12.2
	2	Linoleoyl-dilinolenoylglycerol	77.3	83.7	7.5	11.1	36.1	66.8	1.3	10.0
	3	Dilinoleoyl-linolenoylglycerol	56.1	41.8	6.0	5.7	15.6	24.2	0.9	3.7
	4	Dilinolenoyl-oleoylglycerol	26.7	31.2	2.5	2.9	13.9	30.5	0.8	4.0
	5	Dilinoleoyl-palmitoylglycerol	31.8	51.6	9.2	19.4	41.6	78.7	1.7	9.2
	6	Trilinolein	14.6	6.7	4.8	2.4	19.0	7.8	0.7	1.4
	7	Linoleoyl-linolenoyl-oleoylglycerol	39.2	28.0	4.4	4.1	13.2	23.0	1.6	4.2
	8	Linoleoyl-linolenoyl-palmitoylglycerol	59.8	69.2	10.7	19.0	24.4	41.5	1.9	6.1
	9	Dilinolenoyl-stearoylglycerol	6.8	9.9	1.7	3.9	9.4	19.9	0.4	2.2
	10	Dilinoleoyl-oleoylglycerol	17.8	7.0	5.8	3.4	12.4	8.9	2.0	2.2
	11	Linolenoyl-dioleoylglycerol	10.9	6.3	2.8	2.2	3.9	7.2	1.8	1.7
	12	Dilinoleoyl-palmitoylglycerol	37.2	25.2	8.1	4.7	18.6	18.2	2.6	3.5
	13	Linoleoyl-linolenoyl-stearoylglycerol	14.9	15.3	2.7	3.3	9.1	17.2	0.8	2.2
	14	Linolenoyl-oleoyl-palmitoylglycerol	31.7	36.3	4.9	3.3	17.2	35.1	2.0	5.2
	15	Linolenoyl-dipalmitoylglycerol	7.5	9.4	1.2	1.4	7.0	13.3	0.5	1.8
	16	Linoleoyl-dioleoylglycerol	9.9	3.6	4.9	1.8	5.4	5.1	2.2	2.1
	17	Dilinolenoyl-stearoylglycerol	8.0	6.0	2.2	0.9	5.2	5.2	0.8	0.9
	18	Linoleoyl-oleoyl-palmitoylglycerol	32.8	26.7	10.8	2.8	21.9	33.6	4.0	6.1
	19	Linolenoyl-oleoyl-stearoylglycerol	5.1	5.8	0.7	0.5	2.8	6.4	1.5	1.3
	20	Linoleoyl-dipalmitoylglcerol	7.9	7.2	5.7	1.1	4.8	6.3	2.8	1.7
	21	Linolenoyl-palmitoyl-stearoylglycerol	2.3	3.0	0.6	0.6	2.5	5.9	0.3	0.7
	22	Triolein	2.8	1.2	4.4	3.0	2.1	2.6	1.5	1.6
	23	Linoleoyl-oleoyl-stearoylglycerol	6.5	5.2	4.3	1.0	6.7	9.0	2.6	2.3

Table 2. contd.

Figure	Peak	Assignment	FCV (USA)	FCV (JPN)	BLY (USA)	BLY (JPN)	BLY (JPN)	ORI (TUR)	DAC (PHI)	SAC (IND)
			(ppm (D.B.))							
3	24	Dioleoyl-palmitoylglycerol	6.7	4.9	8.7	1.9	3.7	5.2	4.8	2.6
	25	Linoleoyl-palmitoyl-stearoylglycerol	2.3	2.4	3.7	0.4	2.0	2.7	1.4	0.7
	26	Linolenoyl-distearoylglycerol	0.2	0.4	0.3	0.2	0.5	1.0	0.2	0.1
	27	Oleoyl-dipalmitoylglycerol	3.1	3.2	9.7	0.8	2.7	3.9	5.6	2.3
	28	Tripalmitin	0.8	0.8	0.2	0.2	0.5	0.7	0.2	0.2
	29	Dioleoyl-stearoylglycerol	1.5	1.0	4.0	0.6	0.9	1.5	1.6	0.9
	30	Linoleoyl-distearoylglycerol	0.3	0.4	0.7	0.1	0.4	0.4	0.7	0.2
	31	Oleoyl-palmitoyl-stearoylglycerol	1.2	1.2	7.3	0.5	1.2	1.8	3.4	1.4
	32	Dipalmitoyl-stearoylglycerol	0.4	0.3	0.2	0.1	0.3	0.5	0.3	0.3
	33	Oleoyl-distearoylglycerol	0.4	0.5	2.2	0.5	0.8	0.9	0.9	0.9
	34	Palmitoyl-distearoylglycerol	0.3	0.2	0.1	0.1	0.4	0.8	0.1	0.2
	35	Tristearin	0.1	0.1	0.1	0.1	0.1	0.1	0.0	0.1
4	1	Cholesterol	56.9	39.7	108.6	144.8	70.4	68.6	115.4	101.6
	2	Stigmasterol	64.2	75.1	104.1	192.4	70.6	52.8	163.6	131.3
	3	Campesterol	136.3	87.8	182.4	187.1	127.2	112.2	164.5	127.7
	4	Sitosterol	68.3	79.3	153.6	125.2	115.0	115.4	118.9	132.3
	5	Cholesteryl linolenate	61.9	37.6	33.6	48.3	22.8	38.6	11.6	28.7
	6	Stigmasteryl linolenate	131.6	93.0	42.1	78.6	31.2	54.9	18.5	41.5
	7	Campesteryl linolenate	115.7	68.5	47.1	60.7	37.2	58.1	13.7	36.1
	8	Sitosteryl linolenate	93.7	83.7	61.3	66.2	54.6	87.5	13.6	53.5
	9	Cholesteryl linoleate	67.7	34.4	28.9	32.5	14.6	22.2	11.9	17.7
	10	Stigmasteryl linoleate	138.2	78.4	39.3	54.3	22.9	32.8	22.1	25.4
	11	Campesteryl linoleate	174.3	87.1	55.1	56.3	33.1	46.1	19.1	30.4
	12	Sitosteryl linoleate	97.3	75.5	46.3	40.4	35.0	51.0	13.6	33.3
	13	Cholesteryloleate	11.6	9.2	6.0	3.4	5.0	8.6	5.7	7.0
	14	Stigmasteryl oleate	13.9	12.2	5.7	3.8	5.4	9.4	8.0	6.7
	15	Cholesteryl palmitate	11.3	8.3	6.3	6.9	4.1	7.0	6.5	6.2
	16	Campesteryl oleate	19.7	15.3	7.8	4.0	7.3	12.1	6.1	8.7
	17	Stigmasteryl palmitate	33.2	27.0	14.0	17.2	10.2	14.3	22.5	13.6
	18	Sitosteryl oleate	17.2	20.8	9.6	4.4	11.2	18.6	6.9	14.2
	19	Campesteryl palmitate	21.6	16.0	8.9	8.7	6.8	10.0	8.5	8.0
	20	Sitosteryl palmitate	14.9	18.4	9.2	7.9	8.1	12.6	6.6	10.1
	21	Cholesteryl stearate	2.7	1.9	1.5	1.7	1.1	2.1	2.0	1.9
	22	Campesteryl stearate	3.1	2.7	1.3	1.9	1.0	1.5	3.5	2.0
	23	Campesteryl stearate	4.0	2.8	1.8	1.7	1.4	2.3	2.3	1.9
	24	Sitosteryl stearate	2.5	2.9	1.6	1.5	1.6	3.1	1.6	2.4
5	1	Lutein	654.4	497.3	29.5	57.8	115.4	222.5	61.0	14.3
	10	Hydroxypheophytin *a*	0.8	0.3	0.6	0.2	5.5	11.8	1.3	1.5
	11	Hydroxypheophytin *a*'	0.7	0.2	0.4	0.0	5.9	13.6	2.9	1.3
	12	Pheophytin *a*	1.2	0.8	0.4	0.0	2.3	5.4	1.3	1.8
	13	Pheophytin *a*'	1.1	0.5	0.3	0.0	2.2	5.4	1.8	1.1
	14	β-carotene	394.1	92.0	468.5	353.3	861.4	877.8	197.4	139.4
	15	Solanachromene	422.5	124.3	583.4	479.2	642.0	425.0	186.0	192.2
	21	Solanesyl hydroxypheophorbide *a*	0.3	0.0	0.3	0.0	19.7	25.2	1.4	0.3
	22	Solanesyl hydroxypheophorbide *a*'	0.0	0.0	0.0	0.0	9.7	11.9	0.0	0.0
	23	Solanesyl pheophorbide *a*	0.6	0.3	0.5	0.0	16.1	18.1	2.8	0.6
	24	Solanesyl pheophorbide *a*'	0.5	0.2	0.6	0.0	17.2	18.5	4.2	0.5

FCV than in BLY. Since the previous report referred to the sharp decrease of free fatty acids, glycolipids, phospholipids and triacylglycerols during curing process (24), the result of this time also corresponded with the decrease of the whole lipids during curing process. Although ORI was characterized by chlorophylls distributed at the lower right of the factor loading plot, no other components seemed to contribute to this unique tobacco leaf. On the whole, while a specific component like solanachromene and pheophytin *a* contributed to a specific type of tobacco leaf, as the non-volatile components with low polarity analyzed in this study were the ester forms, the decrease of ester moieties and the degradation of fatty acids during curing process were observed in the result of multivariate analysis. These components were therefore considered predominantly related to the curing process of tobacco leaves.

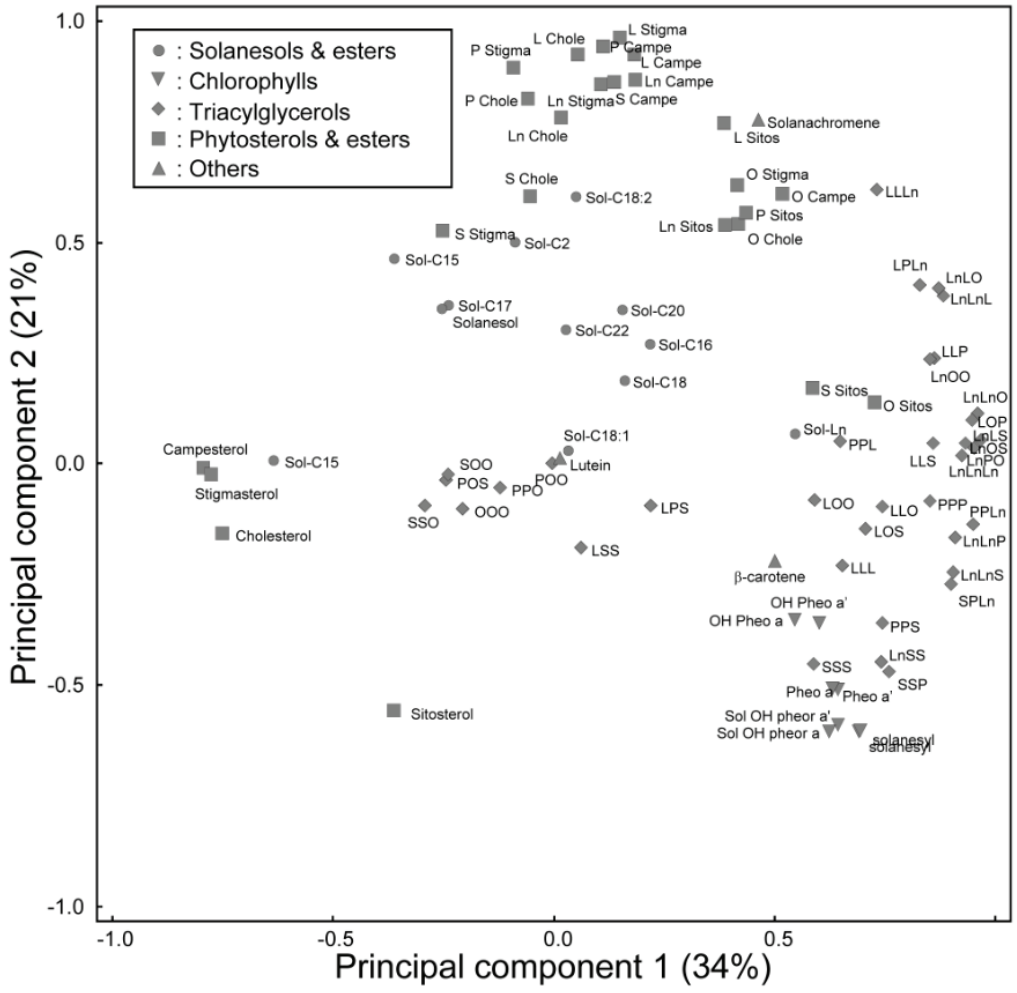

Figure 8. Factor loading plot of principal component analysis of various tobacco leaves. Factor loading plot consists of principal component 1 and 2. The analyzed components are shown in the different shape of mark in the plot. All the names of components are abbreviated in the manner described in abbreviation part. The details of multivariate analysis are described in the "Data processing and multivariate analysis" of "Materials and methods".

CONCLUSIONS

Quantification methods using NARPC hyphenated with PDAD and APCI-MSD have been developed as useful techniques to simultaneously separate, directly detect, and quantify the previously unknown non-volatile components with low polarity in tobacco leaf. The study began with the consolidation of each quantification result in each sample and the execution of multivariate analysis to observe the categories of tobacco leaves and determine the key non-volatile components with low polarity highly related to taste, aroma, species, cultivars, curing processes, and growing districts ofbased on categorized tobacco leaves. PCA and hierarchical clustering analysis showed that non-volatile components with low polarity mainly classified the

tobacco leaves with different curing processes into three categories. While FCV and ORI were basically characterized by phytosteryl esters, solanesyl esters and triacylglycerols including unsaturated higher fatty acids, BLY in addition to DAC and SAC seemed to be contributed by free phytosterols and to contain less amounts of ester components. Although solanachromene and chlorophylls clearly contributed to FCV and ORI, respectively, the overall tendency regarding non-volatile components with low polarity in tobacco leaf was the decrease of ester forms indicating the consumption of energy sources during curing process. Although this study only gave the key components for tobacco leaves with different polarity, the author truly believes that the expansion of targeted resin components, the further number of various tobacco samples and the development of analytical method will lead to more understanding on the complexity and uniqueness of tobacco leaves.

ACKOWLEDGEMENTS

The author was supported by the Tobacco Science Research Center, Japan Tobacco Inc. Technical advice and long support for this study in addition to the previous researches received from H. Kitami, M. Yokoi, Y. Gohara, T. Kashima, M. Yoshizaki, M. Sugano, and K. Aso are gratefully acknowledged.

REFERENCES

1. Voges, E.: Tobacco Encyclopedia; Tobacco Journal International, Virginia, USA, 1984.
2. Davis, D. and M.T. Nielsen: Tobacco: Production, Chemistry, and Technology; edited by D. Davis and M.T. Nielsen, Blackwell Science, Oxford, UK, 1999.
3. Rodman, A. and T.A. Perfetti: The Chemical Components of Tobacco and Tobacco Smoke; CRC Press, Boca Raton, FL, USA, 2008.
4. Leffingwell, J.C.: Basic Chemical Constituents of Tobacco Leaf and Differences among Tobacco Types; in: Tobacco: Production Chemistry and Technology; edited by D. Davis and M.T. Nielsen, Blackwell Science, Oxford, UK, 1999, pp. 265–284.
5. Stedman, R.L.: The Chemical Composition of Tobacco and Tobacco Smoke; Chem. Rev. 68 (1968) 153–207.
6. Schmeltz, I. and D. Hoffmann: Nitrogen-Containing Compounds in Tobacco and Tobacco Smoke; Chem. Rev. 77 (1977) 295–311.
7. Rowland, R.L., P. H. Latimer, and J. A. Giles: Flue-Cured Tobacco. I. Isolation of Solanesol, an Unsaturated Alcohol; J. Am. Chem. Soc. 18 (1956) 4680–4683.
8. Rowland, R.L. and P. H. Latimer: Flue-Cured Tobacco. IV. Isolation of Solanesol Esters; Tob. Sci. 3 (1959) 1–3.
9. Ishida, N.: A Novel Method for Analyzing Solanesyl Esters in Tobacco Leaves Using Atmospheric Pressure Chemical Ionization/Mass Spectrometer; J. Chromatogr. A 1217 (2010) 5794–5801.
10. Davis, D.L.: Waxes and Lipids in the Leaf and Their Relationship to Smoking Quality and Aroma; Rec. Adv. Tob. Sci. 2 (1976) 80–106.
11. Parris, N.A.: Non-Aqueous Reversed-Phase Liquid Chromatography: A Neglected Approach to the Analysis of Low Polarity Samples; J. Chromatogr. A 157 (1978) 161–170.
12. Kadam, M. and D.N. Bhowmick: HPLC Analysis of Rice Bran Oil; J. Food Lipids 13 (2006) 354–361.
13. Cunha, S.C., S. Casal, M.B.P.P. Oliveira: Triacylglycerol Profile by HPLC/ELSD as a Discriminant Parameter of Varietal Olive Oils from Portugal; Ital. J. Food Sci. 17 (2005) 447–454.
14. Amaral, J.S., S.C. Cunha, A. Santos, M.R. Alve, R.M. Seabra, M.B.P.P. Oliveira: Influence of Cultivar and Environmental Conditions on the Triacylglycerol Profile of Hazelnut (*Corylus avellana* L.); J. Agric. Food Chem. 54 (2006) 449–456.
15. Amaral, J.S., S.C. Cunha, M.R. Alves, J.A. Pereira, R.M. Seabra, and M.B.P.P. Oliveira: Triacylglycerol Composition of Walnut (*Juglans regia* L.) Cultivars: Characterization by HPLC-ELSD and Chemometrics; J. Agric. Food Chem. 52 (2004) 7964–7969.
16. Türkan, A. and Ş. Kalay: Monitoring Lipase-Catalyzed Methanolysis of Sunflower Oil by Reversed-Phase High-Performance Liquid Chromatography: Elucidation of the Mechanisms of Lipases; J. Chromatogr. A 1127 (2006) 34–44.
17. Holcapek, M., P. Jandera, P. Zderadička, and L. Hrubá: Characterization of Triacylglycerol and Diacylglycerol Composition of Plant Oils Using High-Performance Liquid Chromatography - Atmospheric Pressure Chemical Ionization Mass Spectrometry; J. Chromatogr. A 1010 (2003) 195–215.
18. Jakab, A., K. Héberger, and E. Forgács: Comparative Analysis of Different Plant Oils by High-Performance Liquid Chromatography-Atmospheric Pressure Chemical Ionization Mass Spectrometry; J. Chromatogr. A 976 (2002) 255–263.
19. Lísa, M., M. Holčapek, T. Řezanka, and N. Kabátová: HPLC/APCI-MS and GC/FID Characterization of Δ5-Olefinic Fatty Acids in Triacylglycerols From Conifer Seed Oils; J. Chromatogr. A 1146 (2007) 67–77.
20. Dugo, P., O. Favoino, P. Q. Tranchida, G. Dugo, and L. Modello: Off-Line Coupling of Non-Aqueous Reversed-Phase and Silver Ion High-Performance Liquid Chromatography-Mass Spectrometry for the Characterization of Rice Oil Triacylglycerol Positional Isomers; J. Chromatogr. A 1041 (2004) 135–142.
21. Lísa, M. and M. Holčapek: Triacylglycerols Profiling in Plant Oils Important in Food Industry, Dietetics and Cosmetics Using High-Performance Liquid Chromatography-Atmospheric Pressure Chemical Ionization Mass Spectrometry; J. Chromatogr. A 1198 (2008) 115–130.
22. Lerma-Garcia, M.J., R. Lusardi, E. Chiavaro, L. Cerretani, A. Bendini, G. Ramis-Ramo, and E.F. Simo-Alfonso: Use of Triacylglycerol Profiles Established by High Performance Liquid Chromatography with Ultraviolet-Visible Detection to Predict the Botanical Origin of Vegetable Oils; J. Chromatogr. A 1218 (2011) 7521–7527.
23. Cai, S., L.C. Short, J.A. Syage, M. Potvin, and J.M.

Curtis: APPI-LC/MS Analysis of Triacylglycerol Lipids - Effects of Mobile Phases on Sensitivity; J. Chromatogr. A 1173 (2007) 88–97.
24. Ishida, N.: A Comprehensive Study on Triacylglycerols in Tobacco Leaves Using Liquid Chromatography and Atmospheric-Pressure Chemical-Ionization Mass Spectrometry; Beitr. Tabakforsch. Int. 25 (2013) 627–637.
25. Ishida, N.: A Method for Simultaneous Analysis of Phytosterols and Phytosterol Esters in Tobacco Leaves Using Non Aqueous Reversed Phase Chromatography and Atmospheric Pressure Chemical Ionization Mass Spectrometry Detector; J. Chromatogr. A 1340 (2014) 99–108.
26. Ishida, N.: Expanded Separation Technique for Chlorophyll Metabolites in Oriental Tobacco Leaf Using Non-Aqueous Reversed Phase Chromatography; J. Chromatogr. A 1218 (2011) 5810–5818.
27. Rowland, R.L.: Flue-Cured Tobacco. III. Solanachromene and α-Tocopherol; J. Am. Chem. Soc. 22 (1958) 6130.

Address for correspondence:

Naoyuki Ishida
Product Technology Development Center
Japan Tobacco Inc.
1-17-7 Yokokawa, Sumida-ku
Tokyo, Japan
E-mail: naoyuki.ishida@jt.com